RESEARCH ARTICLE

Identification of de novo mutations for *ARID1B* haploinsufficiency associated with Coffin–Siris syndrome 1 in three Chinese families via array-CGH and whole exome sequencing

Guanting Lu[1*†] , Qiongling Peng[2†], Lianying Wu[1], Jian Zhang[1] and Liya Ma[2*]

Abstract

Background: Coffin–Siris syndrome (CSS) is a multiple malformation syndrome characterized by intellectual disability associated with coarse facial features, hirsutism, sparse scalp hair, and hypoplastic or absent fifth fingernails or toenails. CSS represents a small group of intellectual disability, and could be caused by at least twelve genes. The genetic background is quite heterogenous, making it difficult for clinicians and genetic consultors to pinpoint the exact disease types.

Methods: Array-Comparative Genomic Hybridization (array-CGH) and whole exome sequencing (WES) were applied for three trios affected with intellectual disability and clinical features similar with those of Coffin–Siris syndrome. Sanger sequencing was used to verify the detected single-nucleotide variants (SNVs).

Results: All of the three cases were female with normal karyotypes of 46, XX, born of healthy, non-consanguineous parents. A 6q25 microdeletion (arr[hg19]6q25.3(155,966,487–158,803,979) × 1) (2.84 Mb) (case 1) and two loss-of-function (LoF) mutations of *ARID1B* [c.2332 + 1G > A in case 2 and c.4741C > T (p.Q1581X) in case 3] were identified. All of the three pathogenic abnormalities were de novo, not inherited from their parents. After comparison of publicly available microdeletions containing *ARID1B*, four types of microdeletions leading to insufficient production of *ARID1B* were identified, namely deletions covering the whole region of *ARID1B*, deletions covering the promoter region, deletions covering the termination region or deletions covering enhancer regions.

Conclusion: Here we identified de novo ARID1B mutations in three Chinese trios. Four types of microdeletions covering ARID1B were identified. This study broadens current knowledge of ARID1B mutations for clinicians and genetic consultors.

---

*Correspondence: guantlv@126.com; maliya226@qq.com
†Guanting Lu and Qiongling Peng have contributed equally to this work
[1] Department of Pathology, Laboratory of Translational Medicine Research, Deyang Key Laboratory of Tumor Molecular Research, Deyang People's Hospital, No. 173 First Section of TaishanBei Road, Jiangyang District, Deyang 618000, China
[2] Department of Child Healthcare, Shenzhen Baoan Women's and Children's Hospital, Jinan University, 56 Yulyu Road, Baoan District, Shenzhen 518000, China

Lu *et al. BMC Medical Genomics*   (2021) 14:270

Page 2 of 14

Background

Coffin–Siris syndrome (CSS, OMIM#135900) is a rare congenital anomaly syndrome characterized by intellectual disability, growth deficiency, microcephaly, coarse facial features and hypoplastic nail of the fifth finger and/or toe [1]. Most of the cases were sporadic and showed an autosomal dominant mode of inheritance. The global prevalence of this disease was estimated at approximately 1:10,000–1:100,000 [2].

According to the available reports, the genetics of CSS is quite heterogenous. Currently, there are 12 types of CSSs caused by pathogenic mutations in different genes: CSS1 (OMIM#135900) by *ARID1B* (OMIM#614556) [2], CSS2 (OMIM#614607) by *ARID1A* (OMIM#603024) [3], CSS3 (OMIM#614608) by *SMARCB1* (OMIM#601607) [4], CSS4 (OMIM#614609) by *SMARCA4* (OMIM#603254) [4], CSS5 (OMIM#616938) by *SMARCE1* (OMIM#603111) [4, 5], CSS6 (OMIM#617808) by *ARID2* (OMIM#609539) [6], CSS7 (OMIM#618027) by *DPF2* (OMIM#601671) [7], CSS8 (OMIM#618362) by *SMARCC2* (OMIM#601734) [8], CSS9 (OMIM#615866) by *SOX11* (OMIM#600898) [9], CSS10 (OMIM#618506) by *SOX4* (OMIM#184430) [10], CSS11 (OMIM#618779) by *SMARCD1* (OMIM#601735) [11], and CSS12 (OMIM#619325) by *BICRA* (OMIM#605690) [12]. It is worth noting that mutations in another gene, *SMARCA2* (OMIM#600014) could lead to Nicolaides–Baraitser syndrome (NCBRS; OMIM#601358), which possessed similar phenotypes with Coffin–Siris syndrome [13–15]. Therefore, it is a great challenge for clinicians to identify the disease types and genetic inheritable patterns. With the application of candidate gene panels and whole exome sequencing (WES), the diagnostic yields have been improved greatly from about 15–20% with chromosomal microarray (CMA) to 35–50% of cases [16–19].

Here, through array-CGH and whole-exome sequencing (WES) techniques, we identified one 2.84 Mbp 6q25 microdeletion in case 1, two loss-of-function (LoF) variants in *ARID1B* (AT-rich interaction domain 1B) in case 2 (c.2332 + 1G > A) and case 3 (c.4741C > T, p.Q1581X) All of the three abnormalities were novel, not inherited from any of their parents. Because more than 10 types of Coffin-Siris syndrome, and many hospitalized patients with intellectual disability (ID) were in their childhood without distinct clinical phenotypes, it is difficult to identify the underlying genetic factors.

The combination of array-CGH and WES might be an efficient methodology to pinpoint the causal mutations.

Methods

Sample collection

This study was conducted in accordance with the Code of Ethics of the World Medical Association (Declaration of Helsinki) for experiments involving humans. This study was approved by the Ethical Committee of the Shenzhen Bao'an Women's and Children's Hospital. Written informed consent was obtained from each individual. The clinical phenotypes were compiled in Table 1.

Peripheral venous blood was collected from the three patients and their parents. Genomic DNA was extracted using the TIANamp Blood DNA Kit (DP348, Tiangen Biotech, Beijing, China) according to the manufacturer's instructions.

Array-comparative genomic hybridization (Array-CGH)

Array-CGH was performed using the Fetal DNA Chip (Version 1.2) designed by The Chinese University of Hong Kong (CUHK) [20, 21]. The chip contains a total of 60,000 probes for more than 100 diseases caused by known microduplication/microdeletions. It doesn't include small-size chromosomal abnormalities, copy number polymorphism, chimerism and chromosomal rearrangement [22]. The experimental procedures were performed according to the standard Agilent protocol (Agilent Oligonucleotide Array-Based CGH for Genomic DNA Analysis, version 3.5). Hybridized slides were scanned with SureScan High-Resolution Microarray Scanner (G2505B, Agilent Technologies, Santa Clara, CA, USA), and the image data were extracted and converted to text files using Agilent Feature Extraction software (Version 10.5.1.1). The data were graphed and analyzed using Agilent CGH Analytics software.

Only gains or losses that encompassed by at least three consecutive oligomers on the array were considered. Then, the clinical relevance of observed chromosomal aberrations was estimated according to data found in the scientific literature and databases for each of the regions and genes involved, using the DECIPHER database for known microdeletion and microduplication syndromes and the Online Mendelian Inheritance in Man (OMIM) for known disease-causing genes, gene functions, and inheritance patterns. DNA copy alterations were considered possibly pathogenic when they involved regions known to be associated with microdeletion or microduplication syndromes.

Lu *et al. BMC Medical Genomics*   (2021) 14:270

Page 3 of 14

Table 1 Clinical information of the three cases

	Case 1 (Family1)	Case 2 (Family 2)	Case 3 (Family 3)
Genetic detection			
ARID1B mutations	−	c.2332 + 1G > A (splicing)	c.4741C > T (p.Q1581X)
arrayCGH	6q25.3 deletion	−	−
Cytogenetic band deleted	46,XX	46,XX	46,XX
General information			
Age at report	3y5m	2y11m	3y
Sex	Female	Female	Female
Birth weight (g)	2950	2650	3200
Birth height (cm)	NA	48	50
Head circumstances (cm)	NA	32	34
Facial features			
Thick hair	+	+	+
Thick eyebrows	+	+	+
Thick eyelashes	+	+	+
Orbital hypertelorism	−	+	−
Down-slanting palpebral fissure	−	+	+
Up-slanting palpebral fissure	−	−	−
Nasal root abnormality	−	+	−
Low set ears	−	−	+
Abnormal ears	−	−	−
Midface hypoplasia	+	+	+
Wide mouth	+	+	+
Long philtrum	−	−	−
Upper lip vermilion feature	−	+	+
Thick lower lip vermilion	−	+	+
Palatal abnormality	−	−	−
Skeletal–limb			
Transverse crease	+	+	+
Clinodactyly	+	−	−
Hypoplastic/absent fifth finger/toe	+	+	−
Hypoplastic/absent nail (fifth finger/toe)	+	+	−
Hypoplastic/absent nail (other fingers/toes)	−	−	−
Broad thumb	−	+	+
Prominent interphalangeal joints	−	−	−
Prominent distal phalanges	−	−	−
Scoliosis/spinal abnormalities	−	+	−
Joint laxity	+	+	+
Nervous system			
Developmental delay	+	+	+
Seizures	−	+	−
Speech delay	+	+	+
Structural brain abnormalities	−	−	−
Agenesis of corpus callosum	−	−	−
Hypotonia	+	+	+
Hypertonia	−	−	−
Abnormal shape of head	+	+	+
Growth restriction	+	+	+
Microcephaly	−	−	−
Others			

Lu *et al. BMC Medical Genomics*   (2021) 14:270

Page 4 of 14

Table 1 (continued)

	Case 1 (Family1)	Case 2 (Family 2)	Case 3 (Family 3)
Hirsutism	−	+	+
Congenital heart defects	−	−	−
Genitourinary defects	−	−	−
Gastrointestinal abnormalities	−	−	−
Sucking difficulty	+	−	+
Feeding difficulty	−	+	+
Frequent vomiting	−	−	−
Hearing impairment	−	+	−
Visual impairment	−	−	−
Recurrent infections	−	−	−
Family information			
Siblings	One sister; normal	One brother; with attention deficit hyperactivity disorder	One brother; normal
Family history	No	No	No
Consanguineous marriage	No	No	No

Whole exome sequencing for the affected trios

To investigate the genetic cause of the disease, WES was performed for the trios of the two affected probands (case 2 and 3) at MyGenostics Co. LTD. Briefly, genomic DNA of each sample was quantified by NanoDrop spectrophotometry 8000 (Thermo Scientific, Waltham, MA, USA). 1 μg of genomic DNA was sheared by nebulization. Sheared DNA were ligated to the 3′ end of Illumina adapters. Products with 350–400 bp were amplified by polymerase chain reaction (PCR). The quality of the amplified products was checked using the Agilent Bioanalyzer (Agilent Technologies, Santa Clara, CA, USA). The amplified DNA was captured with Gencap Human whole Exon Kit (52 M) based on MyGenostics GenCap™ Enrichment Technologies (MyGenostics, Beijing, China). The capture procedure was performed according to the manufacturer's protocol. Finally, the resultant libraries were sequenced on Illumina HiSeq 2500 platform for paired-end sequencing.

The sequencing depth was about $100\times$ for each sample. Sequences were aligned to the human reference genome (UCSC hg19). ANNOVAR was applied to annotate the VCF file. Variants with a Minor Allele Frequency (MAF) > 0.1% or synonymous single nucleotide variants (SNVs) were removed. SNVs causing splicing, frameshift, stop gain or stop loss were kept for subsequent analysis. The location, type, conservation of the identified mutations was obtained from several public databases, such as UCSC Genome Browser, NCBI dbSNP, NCBI ClinVar, 1000 Genome and ExAC. The pathogenicity of the variants was evaluated according to the American College of Medical Genetics and Genomics (ACMG) guidelines [23] and the online software, PolyPhen-2 and SIFT for functional prediction. A position was called as heterozygous if 25% or more of the reads identify the minor allele.

Protein interaction analysis

The 12 genes for CSS and 1 for NCBRS listed in OMIM were used as input to STRING Protein–Protein interaction database (http://string-db.org/), that holds experimental, predicted and transferred interactions together with interactions obtained through text mining [24]. To select stronger interactors, network clustering was performed using k-means algorithm (number of clustering was set as 4).
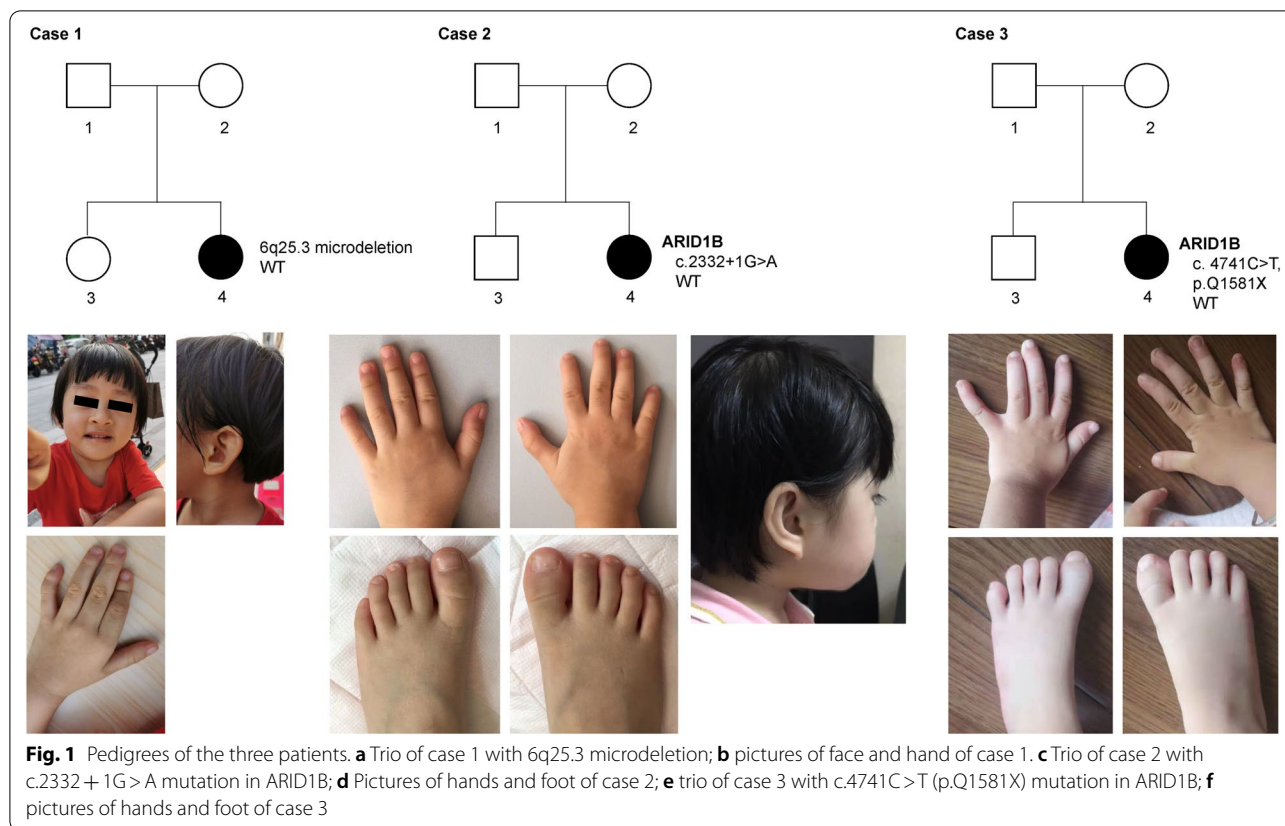
Results

Clinical and demographic characteristics of three cases

Case 1 (Family 1)

The girl was G2P2, born by cesarean section at full-term of pregnancy. The birth weight was 2.95 kg. At 1 year 6 months old, the child was unbale to speak, but not taken to seek medical advice. It was at the age of nearly 2 that the child could unconsciously made a "Baba-Mama" sound. At 2 years 4 months old, she was still unable to walk without support. Now, she was 3 years and 5 months old, with a weight at 11.9 kg, height 88 cm, and head circumstance 48.5 cm. The pedigree and some features were depicted in Fig. 1a and b. Family history: Her parents were healthy and non-consanguineous. Her mother was 30 years old and had a healthy living style during pregnancy. The patient has a healthy 6-year-old sister.

Case 2 (Family 2)

The girl was G5P2A3, born by cesarean section at 39 + 3 weeks of gestation, with a birth weight of 2.65 kg,

Lu *et al. BMC Medical Genomics*   (2021) 14:270

Page 5 of 14

Fig. 1 Pedigrees of the three patients. **a** Trio of case 1 with 6q25.3 microdeletion; **b** pictures of face and hand of case 1. **c** Trio of case 2 with c.2332 + 1G > A mutation in ARID1B; **d** Pictures of hands and foot of case 2; **e** trio of case 3 with c.4741C > T (p.Q1581X) mutation in ARID1B; **f** pictures of hands and foot of case 3

birth height 48 cm and head circumference 32 cm. Two months after birth, she was admitted to the Shenzhen Hospital affiliated to the University of Hong Kong for treatment due to five times of "suspicious convulsions " and diagnosed as "epilepsy". At 5 months old, her height increased to 90 cm, and weight to 11.6 kg. Her psychomotor development was significantly behind the children of the same age, and also combined with hypotonia. The pedigree and some features were depicted in Fig. 1c and d. Family history: Her healthy parents were not consanguineous. Her mother was 38 years old and had no history of smoking, drinking, long-term exposure to chemicals and harmful radiation during pregnancy. The patient has a 12-year-old brother suffered from "attention deficit hyperactivity disorder".
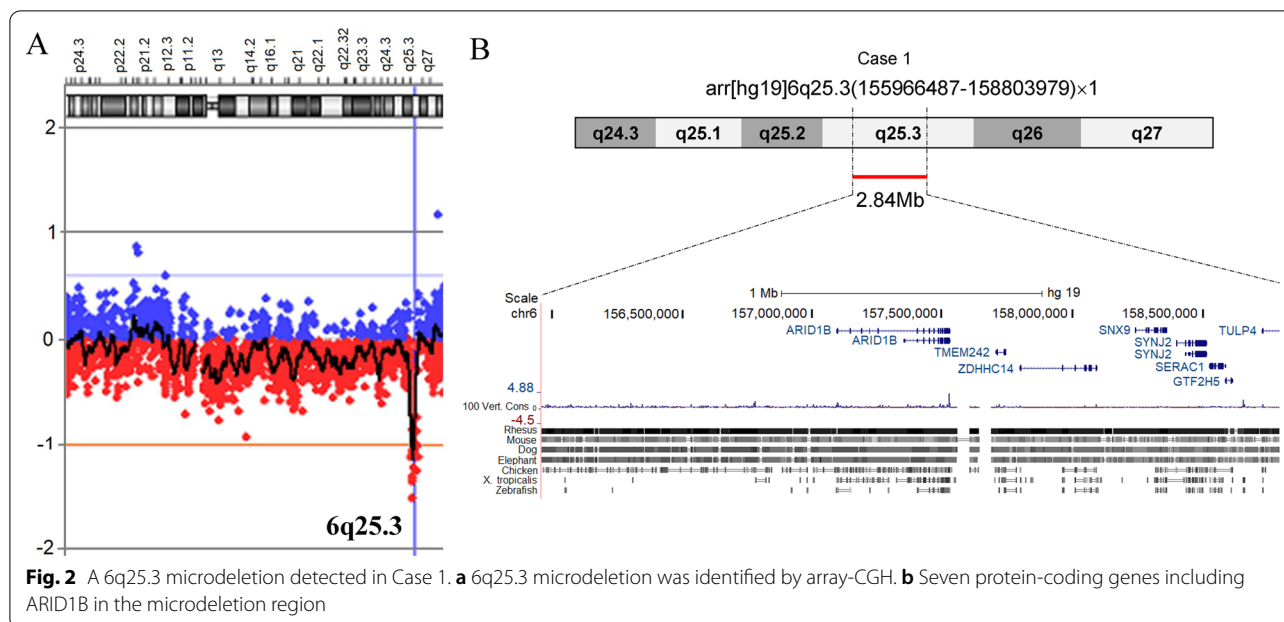
Case 3 (Family 3)

The girl was G2P2, born naturally at 39 + 1 weeks of gestation with a birth weight of 3.2 kg, height 50 cm and head circumference 34 cm. Her crying voice was weak at birth. She could not take the initiative to suck in the first two months after birth and was fed with dropper. On the 4th day after birth, she was hospitalized for 1 week due to "neonatal hyperbilirubinemia". About 1 year ago (at 8 months and 21 days old), the child could not sit alone

and was treated as "developmental delay". Her cognitive and motor development was significantly lagging behind children of the same age. She could understand and execute simple instructions, and uttered no more than 5 words. At this time, her height was 94 cm, with a weight at 12.4 kg. The pedigree and some features were depicted in Fig. 1e and f. Family history: She was born of healthy, non-consanguineous parents. Her mother was 35 years old and had no history of smoking, drinking, long-term exposure to chemicals and harmful radiation during pregnancy. The patient has a healthy brother.

Clinical characters of the facial, skeletal–limb, nervous system and other features of the three cases were compiled in Table 1.

A 6q25 microdeletion was identified in case 1 by array-CGH

Oligonucleotide array-CGH was performed for the three patients using the Fetal DNA Chip (Version 1.2) designed by the Chinese University of Hong Kong (CUHK). A microdeletion at 6q25.3 was detected in case 1, arr[hg19]6q25.3(155,966,487–158,803,979) × 1. The length of this microdeletion was about 2.84 Mbp (chr6:155,966,487–158,803,979) (Fig. 2a). This deletion was not identified in her parents. Besides, there were no deletions or duplications detected in case 2 and case 3.

Lu *et al. BMC Medical Genomics*   (2021) 14:270

Page 6 of 14

Fig. 2 A 6q25.3 microdeletion detected in Case 1. **a** 6q25.3 microdeletion was identified by array-CGH. **b** Seven protein-coding genes including ARID1B in the microdeletion region

This deleted region contains 7 protein-encoding genes, and is highly conserved in mammals (Fig. 2b). Five of them (*ARID1B, ZDHHC14, SNX9, SYNJ2* and *GTF2H5*) were localized on the sense strand and two (*TMEM242* and *SERAC1*) on the antisense strand.

Two novel pathological point mutations were identified by WES

As for the other two cases, WES was performed at MyGenostics (MyGenostics, Beijing, China). The aligned bases for case 2 and case 3 were 13,859.9 and 15,678.15 Mb, respectively. The ratios of the coverage on target regions were 99.33% and 99.69%, respectively. The average sequencing depths on target regions were 109.65 and 118.64 for case 2 and case 3, respectively.

In case 2, a heterozygous SNV was detected at the splicing donor site of exon 6 (c.2332 + 1G > A, chr6:157,431,696) of *ARID1B* (NM_017519) (Fig. 3a, Table 2). It had been confirmed by Sanger sequencing (Fig. 3b). After comparing the sequences from human, chimpanzee, rhesus, cow, dog, mouse, rat and X. tropicalis, this nucleotide (2332 + 1G) was strongly conserved during evolution. This SNV was not detected in the several public genomic databases, such as 1000Genome Project (n = 2504), NHLBI Exome Sequencing Project (GO-ESP) (n = 6503), The Exome Aggregation Consortium (ExAC) (n = 60,706), gnomAD (n = 15,708) and NHLBI Trans-Omics for Precision Medicine (TOPMED) (n = 60,000). Besides, this mutation was not identified in the parents' genomes. Therefore, this mutation was appeared spontaneously in case 2 and should be regarded as 'de novo'. According to criteria of ACMG guidelines, this SNV was classified as PVS1 + PS2 + PM2 and annotated as "Likely pathogenic".

In case 3, a nonsense mutation (c.4741C > T, chr6:157,522,259) was identified in the exon 18 of *ARID1B* (NM_017519), causing the codon (CAG) for Gln (Q) to be a premature stop codon (TAG, X) (p.Q1581X) (Fig. 3a, d, Table 2). This mutation was verified by Sanger sequencing (Fig. 3c). This nucleotide (4492C) was strongly conserved during evolution. The mutation was not included in the large-scale genomic databases mentioned above. Since this stop gain mutation was only identified in case 3 and not in her parents, it was regarded as another 'de novo' variant. Besides, the variant has been annotated as rs1554235831 in NCBI dbSNP database. According to the criteria of ACMG guidelines, p.Q1581X was classified as PVS1 + PS2 + PM2 and annotated as "pathogenic".

6q25 Microdeletions involving ARID1B

9 reported 6q25 microdeletions associated with *ARID1B*-related disorders were recruited from published articles. We also collected individuals with developmental disorders whose genomes containing microdeletions involving *ARID1B* gene from DECIPHER [25, 26] and Developmental Delay [27, 28]. 32 were from DECIPHER and 5 from Developmental Delay. The microdeletions were compared against human genome (hg19) using UCSC Genome Browser. Totally, 46 microdeletions were recruited for the subsequent analysis (Fig. 4a). 39 of them were completely (or almost) covered the whole

Lu *et al. BMC Medical Genomics*   (2021) 14:270

Page 7 of 14

Fig. 3 Two de novo mutations of ARID1B gene in case 2 and case 3. **a** Genomic structure of ARID1B gene; Thin box represents exons, line represents introns. **b** Sanger sequencing of the two single-nucleotide mutations. **c** Conservational analysis of the sequences around the two mutations in different organisms. **d** Location of the p.Q1581X in the protein sequence of ARID1B

genomic region of *ARID1B*. As for the remaining partially-covered microdeletions, the shortest one (270,613, chr6:157,096,761–157,101,867) was only 5.11 Kb, just spanning the promoter region of *ARID1B*, just as the deletions reported by Ronzoni L in 2016 and detected in two DECIPHER samples (282,767 and 360,703). There also existed a 28.79 Kb microdeletion (274,690, chr6:157,527,273–157,556,065), which covered the whole last exon of *ARID1B*, thus removing part of the protein coding sequence and the complete 3'-untranslated region (3'-UTR) of *ARID1B*. Interestingly, the microdeletion (266,355, chr6:157,261,502–157,336,055) located in the fifth intron and did not affect the protein coding region of *ARID1B*. According to the chromatin modification patterns from 7 cell lines (GM12878, H1-hESC, HSMM, HUVEC, K562, NHEK and NHLF) from ENCODE (Encyclopedia of DNA Elements) [29], several candidate enhancers were located in the region covered by this deletion (266,355) (Fig. 4b).

Discussion

Currently, there are 12 genes responsible for CSSs and 1 for NCBRS, a disorder with similar phenotypes of CSSs. Among the 13 genes, except the two transcription factors, SOX4 and SOX11, proteins encoded by the remaining 11

genes were bound with each other (Fig. 5a) to form two SWI/SNF-related complex, BAF (Brg/Brahma-associated factors) complex and/or PBAF (Polybromo BRG1 Associated Factor) (Fig. 5b, c). The SWI/SNF complex was originally referred to as the protein complex critical for cellular responses to mating-type switching (SWI) or sucrose fermentation (SNF) in yeast [30, 31]. This multi-protein complex contains more than 15 subunits to activate gene expression through its capacity to remodel and remove nucleosomes at gene promoters [32]. Recently, mutations, translocations and deletions of the subunits in the SWI/SNF complex have been linked to a number of human diseases, such as cancer [33], different types of CSS [4, 34–38] and NCBRS [15].

The gene for CSS1 is *ARID1B* [2, 4, 39], a core subunit of the BAF complex. This gene is the most frequently mutated genes in cases with CSS [5]. The phenotypes caused by *ARID1B* mutations encompass a spectrum of features, including feeding difficulties, laryngomalacia, speech delay, motor delay, hypertrichosis, and cryptorchidism [40]. According to the Human Protein Atlas, ARID1B is expressed ubiquitously, and abundantly detected in never, endocrine, muscle and lymphoid systems (Fig. 5d). It is reported that meticulous coordination between the actin cytoskeleton and the microtubule

Table 2 De novo mutations of ARID1B identified in two cases

Cases	Sex	Location (GRCh37/hg19)	Nucleotide	Amino acid	Zygosity	dbSNP ID	Origin	ACMG	Population frequencies	Impact
2	Female	chr6:157,431,696	c.2332 + 1G > A	–	Het	–	De novo	PVS1 + PS2 + PM2	–	Splicing donor loss
3	Female	chr6:157,522,259	c.4741C > T	p.Q1581X	Het	rs1554235831	De novo	PVS1 + PS2 + PM2	–	Stop gain

Het, heterozygous; X, stop codon; PVS1, pathogenic very strong, represent "loss-of-function"; PS2, pathogenic strong, represent "de novo"; PM2; pathogenic moderate, 2 represent "absent from controls"
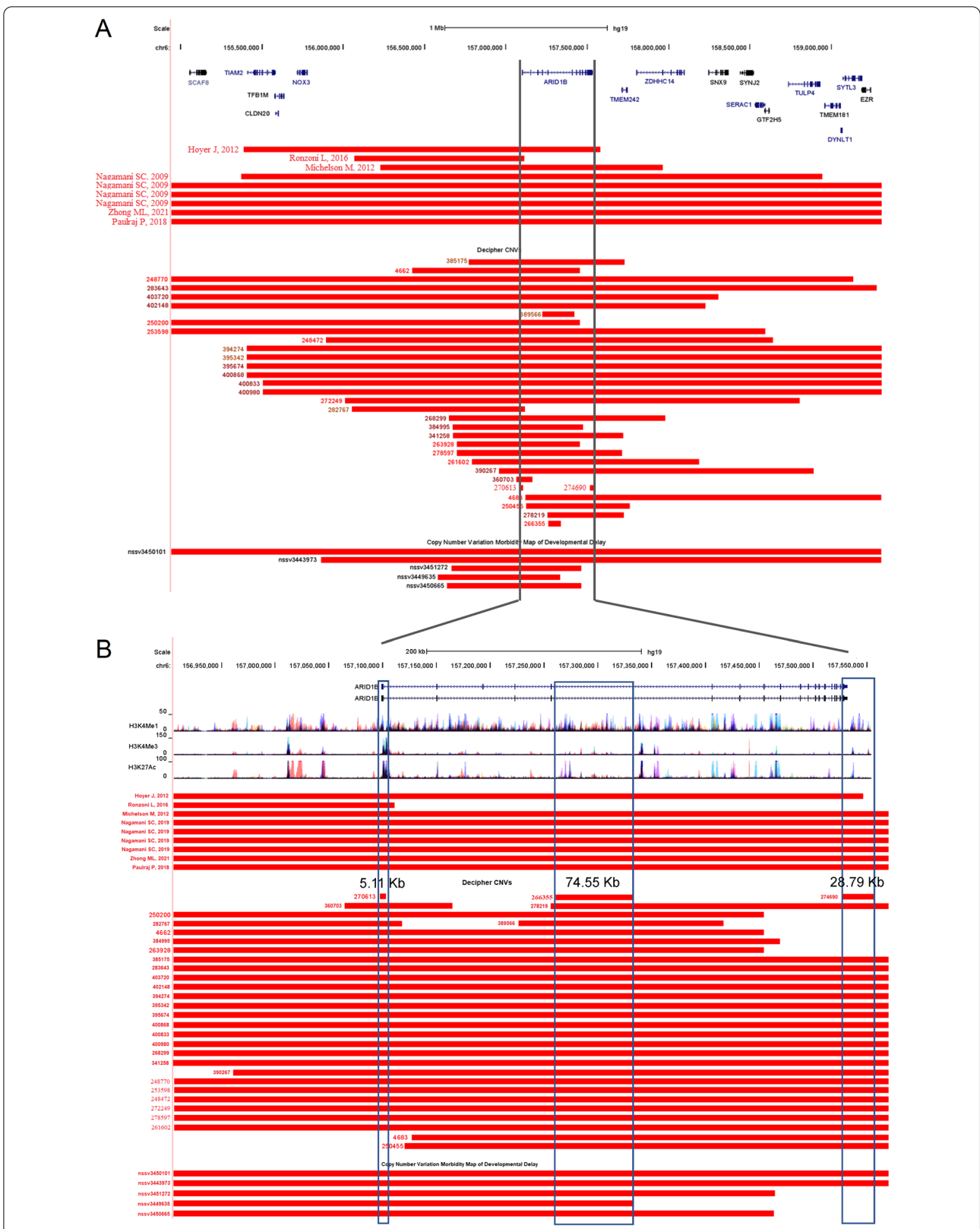
Fig. 4 Mapping of microdeletions involving ARID1B. **a** Mapping of the microdeletions involving ARID1B. **b** Zoomed-in view of the microdeletions. Red bar represents microdeletions

Lu *et al. BMC Medical Genomics*   (2021) 14:270

Page 10 of 14

Fig. 5 Interaction of proteins for CSS and structures of SWI/SNF-related proteins. **a** Interactions of the 12 proteins for Coffin–Siris syndrome and 1 for NCBRS. **b** Structures of BAF. **c** Structures of PBAF. **d** Expression of ARID1B in different tissues of human (adopted from the Human Protein Atlas)
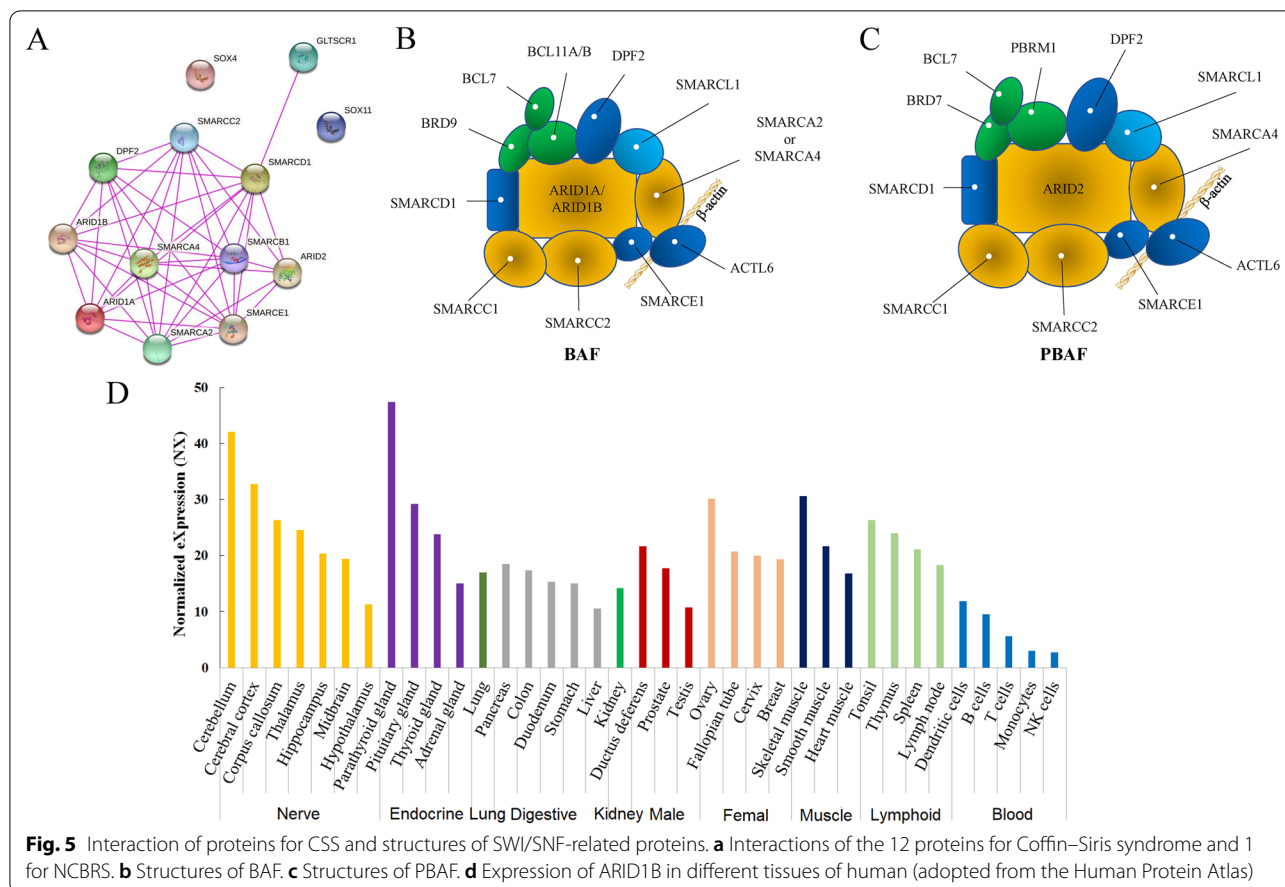
network regulate the formation and transportation of secretory vesicles for proper neurite outgrowth and maintenance, which is critical for normal neural development [41]. This finely-tuned coordination is regulated by the BAF complex [42]. ARID1B (previously named as BAF250B) is a core member of the BAF complex and plays an essential role for dendrite outgrowth and arborization in cortical and hippocampal pyramidal neurons during brain development in mice [43]. ARID1B deficiency led to decreased dendritic branching, thus hinder the dendritic innervation into cortical layer I to form proper synapses. This might disrupt the balanced excitatory and inhibitory inputs and result in pathologic phenotypes of ID.

ARID1B is the crucial pathogenic factor behind 6q25 microdeletion-related disorder

In our case 1, there exists a heterozygous microdeletion arr[hg19]6q25.3(155,966,487–158,803,979) × 1 (Fig. 3a). This region contains 7 protein-coding genes, namely, *ARID1B, TMEM242, ZDHHC14, SNX9, SYNJ2, SERAC1* and *GTF2H5*. It is worth noting that several inheritable disease-causing genes were recruited in the OMIM database. *ARID1B* (OMIM#614556) is the causal gene for CSS1 (OMIM#135900). *GTF2H5* (general transcription factor IIH subunit 5, OMIM#608780) could result in the photosensitive trichothiodystrophy-3 (TTD3) (OMIM#616395) [44–46], a rare autosomal recessive disorder characterized by brittle sulfur-deficient hair, ichthyosis, developmental disabilities, decreased fertility, ocular abnormalities, short stature, and infections [47]. *SERAC1* (serine active site containing 1, OMIM#614725) functions in phosphatidylglycerol remodeling that is essential for mitochondrial function and intracellular cholesterol trafficking [48]. Bi-allelic Mutations of this gene were associated with 3-methyl-glutaric aciduria, accompanied with deafness, encephalopathy and Leigh-like syndrome (MEGDHEL, OMIM#614739) [48–50]. *TMEM242* was reported to affect the assembly of the ATP synthase and mitochondrial complex I, to a certain degree [51]. *ZDHHC14* (zinc finger DHHC-type palmitoyl transferase 14) is highly expressed in the hippocampus and is the only palmitoyl acyltransferase (PAT) predicted to bind Type-I PDZ domain-containing Membrane-associated Guanylate Kinase PSD93, which localizes to the axon initial segment (AIS) [52]. Loss of *ZDHHC14* decreases

outward currents and increases action potential firing in hippocampal neurons. SNX9 (Sorting nexin 9), a member of the sorting nexin family, is required for membrane remodeling during endocytosis [53]. As for *SYNJ2* (synaptojanin 2), it is a ubiquitously expressed phosphoinositol 5-phosphatase, involved in vesicular trafficking and actin dynamics. Although it is not clear whether SYNJ2 played a role in the normal brain development, an association study showed that SYNJ2 was associated with general memory and general cognitive ability [54].

Based on the above analysis, *ARID1B, GTF2H5, SERAC1* and *ZDHHC14* might be the promising candidates responsible for the 6q25 microdeletion syndrome. Currently, there are more than 10 reported individuals harboring 6q25 microdeletion [2, 55–59]. The reported shortest 6q25 deletion (1.1 Mb, chr6:156,004,307–157,120,089) contained only one protein-coding gene, *ARID1B* [60]. According to the ARID1B-related deletions collected in DECIPHER and Developmental Delay, the shortest deletion (270,613) was only 5.11 Kb, just spanning the promoter region and first exon of ARID1B. This deletion made *ARID1B* unable to start the transcription, just as the deletions reported by Ronzoni L in 2016 and detected in two DECIPHER samples (282,767 and 360,703). There also existed a 28.79 Kb microdeletion (274,690), which covered the whole last exon of *ARID1B*, thus removing part of the protein-coding sequence and the complete 3′-UTR of *ARID1B*. The transcription of ARID1B could not stop at the normal termination site, and might produce truncated proteins without the C-terminal BAF250_C domain (pfam12031). Interestingly, the microdeletion (266,355) just located in the middle of *ARID1B*, just like the sample 389,566. According to the chromatin modification patterns from 7 cell lines (GM12878, H1-hESC, HSMM, HUVEC, K562, NHEK and NHLF) from ENCODE, several candidate enhancers were located in this region (Fig. 5b). Loss of these enhancers might affect the transcription efficiency of *ARID1B*. Therefore, the insufficient production of ARID1B could be caused by four types of 6q25 microdeletions, namely whole genomic region, promoter region, termination region and enhancer regions.

Haploinsufficiency of *ARID1B* has been reported to be recurrently detected in intellectual disability (ID) or mental retardation (MRT) [60, 61], therefore, *ARID1B* might be the crucial pathogenic factor behind the 6q25 microdeletion syndrome.

Haploinsufficiency of ARID1B caused by de novo SNVs
In case 2, a variant at the splicing site of exon 6 (c.2332 + 1G > A) of *ARID1B* (NM_017519) was identified. This variant disrupted the splicing donor site (GT) of intron 6, which might affect the proper splicing of *ARID1B*'s mRNA during transcription to produce abnormal transcripts, thus to inactivate the function of ARID1B. It is reported that heterozygous mutations of splicing sites could affect splicing and lead to haploinsufficiency of the affected genes [62, 63]. Therefore, it is reasonable that c.2332 + 1G > A mutation might be detrimental the proper splicing and result to insufficient expression of *ARID1B*.

In case 3, the mutation (c.4741C > T) was located in exon 18 of ARID1B, causing the codon (CAG) for Q to be a premature termination codon (TAG) (p.Q1581X). The transcript contains two stop codons (one at position 1581 and another at position 2237). It had been reported that mRNAs containing premature termination codons (PTC) could be detected and degrade rapidly by a special mRNA surveillance mechanism, Nonsense-mediated mRNA decay (NMD). It is widely accepted that the biological purpose of NMD is to protect cells from potential harmful effects caused by truncated translational products as a consequence of frameshift or nonsense mutations or by inaccurate pre-mRNA splicing [64–66]. It is been found that in 143 patients with CSS, all pathogenic variants were truncating (nonsense, frameshift, splice-site, and deletions of various numbers of exons including whole-gene deletions). Therefore, these two de novo single nucleotide variants in our project might lead to haploinsufficiency of ARID1B and be pathogenic for CSS.

Treatments for ARID1B-related disorders
Till now, there has no effective treatments for ARID1B-related disorders. The present methods are symptomatic treatment and cannot cure this disease. Currently, a clinical trial is ongoing to investigate the effects of clonazepam on children with ARID1B-related intellectual disability in Netherlands (EudraCT: 2019-003558-98). The purpose of this clinical trial is to test the beneficial effects of clonazepam on behavior and cognitive function in ARID1B patients.

Animal with ARID1B haploinsufficiency (Arid1b$^{+/-}$) would be promising models for the study of molecular mechanism and discovering of drugs for ARID1B-related disorder. The Arid1b$^{+/-}$ C57BL/6J mice showed reduced corpus callosum size, dentate gyrus size, cortex thickness, and proliferation [67–69]. It was found that deficiency of GHRH–GH–IGF1 axis was detected in Arid1b$^{+/-}$ mice [67]. Exogenous GH supplementation could significantly reverse the growth retardation in Arid1b$^{+/-}$ mice, but no improvement on abnormal behavioral phenotypes such as anxiety. This indicated there might be other critical unknown druggable targets for the treatment of ARID1B-related disorder. Or Arid1b$^{+/-}$ mice might not be the most suitable animal for the study of ARID1B-related disorder.

Lu *et al. BMC Medical Genomics*   (2021) 14:270

Page 12 of 14

Conclusions

Here we identified a patient with haploinsufficiency of ARID1B caused by a 2.84 mb 6q25 microdeletion and two caused by loss-of-function (LoF) mutations of *ARID1B*. All of the three abnormalities were acquired spontaneously. *ARID1B* gene was the critical genetic factor for ARID1B-related disorder. Besides, four types of 6q25 microdeletion were identified by silico analysis. This would broaden the knowledge about *ARID1B* mutation spectrum for clinicians and genetic counselor.

Abbreviations

CSS: Coffin–Siris syndrome; LoF: Loss-of-function; NCBRS: Nicolaides–Baraitser syndrome; SWI/SNF: Mating-type switching (SWI) or sucrose fermentation (SNF); ARID1B: AT-rich interaction domain 1B; Array-CGH: Array-comparative genomic hybridization; CUHK: Chinese University of Hong Kong; MAF: Minor allele frequency; OMIM: Online Mendelian inheritance in man; WES: Whole-exome sequencing; SNVs: Single nucleotide variants; ExAC: The exome aggregation consortium; ESP: NHLBI exome sequencing project; GTF2H5: General transcription factor IIH subunit 5; TTD3: Trichothiodystrophy-3; SERAC1: Serine active site containing 1; MEGDHEL: 3-Methyl-glutaric aciduria, accompanied with deafness, encephalopathy and Leigh-like syndrome; ZDHHC14: Zinc finger DHHC-type palmitoyl transferase 14; PAT: Palmitoyl acyltransferase; AIS: Axon initial segment; SNX9: Sorting nexin 9; SYNJ2: Synaptojanin 2; ID: Intellectual disability; MRT: Mental retardation; PTC: Premature termination codons; NMD: Nonsense-mediated mRNA decay.

Availability of data and materials

The datasets about whole exome sequencing used for the current study were available at https://www.ncbi.nlm.nih.gov/sra/?term=PRJNA777349.

Declarations

Ethics approval and consent to participate

This study was conducted in accordance with the Code of Ethics of the World Medical Association (Declaration of Helsinki) for experiments involving humans. This study was approved by the Ethical Committee of the Shenzhen Baoan Women's and Children's Hospital. We obtained written informed consent from all individual members included in the study. As for the minors, written informed consent was obtained from the parents or legal guardians.

Consent for publication

Written informed consent was obtained from the patients for publication of this Case report and any accompanying images. A copy of the written consent is available for review by the Editor of this journal. As for the minors, written informed consent was obtained from the parents or legal guardians.

Competing interests

The authors declare that they have no competing interests.

References

1. Vergano SS, Deardorff MA. Clinical features, diagnostic criteria, and management of Coffin–Siris syndrome. Am J Med Genet Part C Semin Med Genet. 2014;166C(3):252–6.
2. Hoyer J, Ekici AB, Endele S, Popp B, Zweier C, Wiesener A, Wohlleber E, Dufke A, Rossier E, Petsch C, et al. Haploinsufficiency of ARID1B, a member of the SWI/SNF-a chromatin-remodeling complex, is a frequent cause of intellectual disability. Am J Hum Genet. 2012;90(3):565–72.
3. Santen GW, Aten E, Vulto-van Silfhout AT, Pottinger C, van Bon BW, van Minderhout IJ, Snowdowne R, van der Lans CA, Boogaard M, Linssen MM, et al. Coffin–Siris syndrome and the BAF complex: genotype-phenotype study in 63 patients. Hum Mutat. 2013;34(11):1519–28.
4. Tsurusaki Y, Okamoto N, Ohashi H, Kosho T, Imai Y, Hibi-Ko Y, Kaname T, Naritomi K, Kawame H, Wakui K, et al. Mutations affecting components of the SWI/SNF complex cause Coffin–Siris syndrome. Nat Genet. 2012;44(4):376–8.
5. Wieczorek D, Bogershausen N, Beleggia F, Steiner-Haldenstatt S, Pohl E, Li Y, Milz E, Martin M, Thiele H, Altmuller J, et al. A comprehensive molecular study on Coffin–Siris and Nicolaides–Baraitser syndromes identifies a broad molecular and clinical spectrum converging on altered chromatin remodeling. Hum Mol Genet. 2013;22(25):5121–35.
6. Shang L, Cho MT, Retterer K, Folk L, Humberson J, Rohena L, Sidhu A, Saliganan S, Iglesias A, Vitazka P, et al. Mutations in ARID2 are associated with intellectual disabilities. Neurogenetics. 2015;16(4):307–14.
7. Vasileiou G, Vergarajauregui S, Endele S, Popp B, Buttner C, Ekici AB, Gerard M, Bramswig NC, Albrecht B, Clayton-Smith J, et al. Mutations in the BAF-complex subunit DPF2 Are associated with Coffin–Siris syndrome. Am J Hum Genet. 2018;102(3):468–79.
8. Machol K, Rousseau J, Ehresmann S, Garcia T, Nguyen TTM, Spillmann RC, Sullivan JA, Shashi V, Jiang YH, Stong N, et al. Expanding the spectrum of BAF-related disorders: de novo variants in SMARCC2 cause a syndrome with intellectual disability and developmental delay. Am J Hum Genet. 2019;104(1):164–78.
9. Tsurusaki Y, Koshimizu E, Ohashi H, Phadke S, Kou I, Shiina M, Suzuki T, Okamoto N, Imamura S, Yamashita M, et al. De novo SOX11 mutations cause Coffin–Siris syndrome. Nat Commun. 2014;5:4011.
10. Zawerton A, Yao B, Yeager JP, Pippucci T, Haseeb A, Smith JD, Wischmann L, Kuhl SJ, Dean JCS, Pilz DT, et al. De novo SOX4 variants cause a neurodevelopmental disease associated with mild dysmorphism. Am J Hum Genet. 2019;104(2):246–59.
11. Nixon KCJ, Rousseau J, Stone MH, Sarikahya M, Ehresmann S, Mizuno S, Matsumoto N, Miyake N, Study DDD, Baralle D, et al. A syndromic neurodevelopmental disorder caused by mutations in SMARCD1, a core SWI/SNF subunit needed for context-dependent neuronal gene regulation in flies. *Am J Hum Genet* 2019, 104(4):596–610.
12. Barish S, Barakat TS, Michel BC, Mashtalir N, Phillips JB, Valencia AM, Ugur B, Wegner J, Scott TM, Bostwick B, et al. BICRA, a SWI/SNF complex member, is associated with BAF-disorder related phenotypes in humans and model organisms. Am J Hum Genet. 2020;107(6):1096–112.
13. Mari F, Marozza A, Mencarelli MA, Lo Rizzo C, Fallerini C, Dosa L, Di Marco C, Carignani G, Baldassarri M, Cianci P, et al. Coffin–Siris and Nicolaides–Baraitser syndromes are a common well recognizable cause of intellectual disability. Brain Dev. 2015;37(5):527–36.
14. Wolff D, Endele S, Azzarello-Burri S, Hoyer J, Zweier M, Schanze I, Schmitt B, Rauch A, Reis A, Zweier C. In-frame deletion and missense mutations of the C-terminal helicase domain of SMARCA2 in three patients with Nicolaides–Baraitser syndrome. Mol Syndromol. 2012;2(6):237–44.

Lu *et al. BMC Medical Genomics*   (2021) 14:270

Page 13 of 14

15. Van Houdt JK, Nowakowska BA, Sousa SB, van Schaik BD, Seuntjens E, Avonce N, Sifrim A, Abdul-Rahman OA, van den Boogaard MJ, Bottani A, et al. Heterozygous missense mutations in SMARCA2 cause Nicolaides–Baraitser syndrome. Nat Genet. 2012;44(4):445–9.

16. Calvo SE, Compton AG, Hershman SG, Lim SC, Lieber DS, Tucker EJ, Laskowski A, Garone C, Liu S, Jaffe DB, et al. Molecular diagnosis of infantile mitochondrial disease with targeted next-generation sequencing. Sci Transl Med. 2012;4(118):118ra110.

17. Cortese A, Wilcox JE, Polke JM, Poh R, Skorupinska M, Rossor AM, Laura M, Tomaselli PJ, Houlden H, Shy ME, et al. Targeted next-generation sequencing panels in the diagnosis of Charcot-Marie-Tooth disease. Neurology. 2020;94(1):e51–61.

18. Kress W, Rost S, Kolokotronis K, Meng G, Pluta N, Muller-Reible C. The genetic approach: next-generation sequencing-based diagnosis of congenital and infantile myopathies/muscle dystrophies. Neuropediatrics. 2017;48(4):242–6.

19. Vasli N, Bohm J, Le Gras S, Muller J, Pizot C, Jost B, Echaniz-Laguna A, Laugel V, Tranchant C, Bernard R, et al. Next generation sequencing for molecular diagnosis of neuromuscular diseases. Acta Neuropathol. 2012;124(2):273–83.

20. Leung TY, Vogel I, Lau TK, Chong W, Hyett JA, Petersen OB, Choy KW. Identification of submicroscopic chromosomal aberrations in fetuses with increased nuchal translucency and apparently normal karyotype. Ultrasound Obstet Gynecol. 2011;38(3):314–9.

21. Huang J, Poon LC, Akolekar R, Choy KW, Leung TY, Nicolaides KH. Is high fetal nuchal translucency associated with submicroscopic chromosomal abnormalities on array CGH? Ultrasound Obstet Gynecol. 2014;43(6):620–4.

22. Iafrate AJ, Feuk L, Rivera MN, Listewnik ML, Donahoe PK, Qi Y, Scherer SW, Lee C. Detection of large-scale variation in the human genome. Nat Genet. 2004;36(9):949–51.

23. Richards S, Aziz N, Bale S, Bick D, Das S, Gastier-Foster J, Grody WW, Hegde M, Lyon E, Spector E, et al. Standards and guidelines for the interpretation of sequence variants: a joint consensus recommendation of the American College of Medical Genetics and Genomics and the Association for Molecular Pathology. Genet Med. 2015;17(5):405–24.

24. Szklarczyk D, Gable AL, Nastou KC, Lyon D, Kirsch R, Pyysalo S, Doncheva NT, Legeay M, Fang T, Bork P, et al. The STRING database in 2021: customizable protein-protein networks, and functional characterization of user-uploaded gene/measurement sets. Nucl Acids Res. 2021;49(D1):D605–12.

25. Swaminathan GJ, Bragin E, Chatzimichali EA, Corpas M, Bevan AP, Wright CF, Carter NP, Hurles ME, Firth HV. DECIPHER: web-based, community resource for clinical interpretation of rare variants in developmental disorders. Hum Mol Genet. 2012;21(R1):R37-44.

26. Bragin E, Chatzimichali EA, Wright CF, Hurles ME, Firth HV, Bevan AP, Swaminathan GJ. DECIPHER: database for the interpretation of phenotype-linked plausibly pathogenic sequence and copy-number variation. Nucl Acids Res. 2014;42(Database issue):D993–1000.

27. Coe BP, Witherspoon K, Rosenfeld JA, van Bon BW, Vulto-van Silfhout AT, Bosco P, Friend KL, Baker C, Buono S, Vissers LE, et al. Refining analyses of copy number variation identifies specific genes associated with developmental delay. Nat Genet. 2014;46(10):1063–71.

28. Cooper GM, Coe BP, Girirajan S, Rosenfeld JA, Vu TH, Baker C, Williams C, Stalker H, Hamid R, Hannig V, et al. A copy number variation morbidity map of developmental delay. Nat Genet. 2011;43(9):838–46.

29. Consortium EP. An integrated encyclopedia of DNA elements in the human genome. Nature 2012;489(7414):57–74.

30. Neigeborn L, Carlson M. Genes affecting the regulation of SUC2 gene expression by glucose repression in *Saccharomyces cerevisiae*. Genetics. 1984;108(4):845–58.

31. Stern M, Jensen R, Herskowitz I. Five SWI genes are required for expression of the HO gene in yeast. J Mol Biol. 1984;178(4):853–68.

32. Kwon H, Imbalzano AN, Khavari PA, Kingston RE, Green MR. Nucleosome disruption and enhancement of activator binding by a human SW1/SNF complex. Nature. 1994;370(6489):477–81.

33. Kadoch C, Hargreaves DC, Hodges C, Elias L, Ho L, Ranish J, Crabtree GR. Proteomic and bioinformatic analysis of mammalian SWI/SNF complexes identifies extensive roles in human malignancy. Nat Genet. 2013;45(6):592–601.

34. Vasko A, Drivas TG, Schrier Vergano SA. Genotype-phenotype correlations in 208 individuals with Coffin–Siris syndrome. Genes. 2021;12(6):937.

35. Mashtalir N, D'Avino AR, Michel BC, Luo J, Pan J, Otto JE, Zullow HJ, McKenzie ZM, Kubiak RL, St Pierre R, et al. Modular organization and assembly of SWI/SNF family chromatin remodeling complexes. Cell. 2018;175(5):1272–88.

36. Mani U, Goutham RNA, Mohan SS. SWI/SNF infobase-an exclusive information portal for SWI/SNF remodeling complex subunits. PLoS ONE. 2017;12(9):e0184445.

37. Schick S, Rendeiro AF, Runggatscher K, Ringler A, Boidol B, Hinkel M, Majek P, Vulliard L, Penz T, Parapatics K, et al. Systematic characterization of BAF mutations provides insights into intracomplex synthetic lethalities in human cancers. Nat Genet. 2019;51(9):1399–410.

38. Srikanth S, Ramachandran S, Mohan SS. Construction of the gene regulatory network identifies MYC as a transcriptional regulator of SWI/SNF complex. Sc Rep. 2020;10(1):158.

39. Zweier M, Peippo MM, Poyhonen M, Kaariainen H, Begemann A, Joset P, Oneda B, Rauch A. The HHID syndrome of hypertrichosis, hyperkeratosis, abnormal corpus callosum, intellectual disability, and minor anomalies is caused by mutations in ARID1B. Am J Med Genet Part A. 2017;173(5):1440–3.

40. van der Sluijs PJ, Jansen S, Vergano SA, Adachi-Fukuda M, Alanay Y, AlKindy A, Baban A, Bayat A, Beck-Wodl S, Berry K, et al. The ARID1B spectrum in 143 patients: from nonsyndromic intellectual disability to Coffin–Siris syndrome. Genet Med. 2019;21(6):1295–307.

41. Tsaneva-Atanasova K, Burgo A, Galli T, Holcman D. Quantifying neurite growth mediated by interactions among secretory vesicles, microtubules, and actin networks. Biophys J. 2009;96(3):840–57.

42. Bachmann C, Nguyen H, Rosenbusch J, Pham L, Rabe T, Patwa M, Sokpor G, Seong RH, Ashery-Padan R, Mansouri A, et al. mSWI/SNF (BAF) complexes are indispensable for the neurogenesis and development of embryonic olfactory epithelium. PLoS Genet. 2016;12(9):e1006274.

43. Ka M, Chopra DA, Dravid SM, Kim WY. Essential roles for ARID1B in dendritic arborization and spine morphology of developing pyramidal neurons. J Neurosci. 2016;36(9):2723–42.

44. Michalska E, Koppolu A, Dobrzanska A, Ploski R, Gruszfeld D. A case of severe trichothiodystrophy 3 in a neonate due to mutation in the GTF2H5 gene: clinical report. Eur J Med Genet. 2019;62(9):103557.

45. Moriwaki S, Saruwatari H, Kanzaki T, Kanekura T, Minoshima S. Trichothiodystrophy group A: a first Japanese patient with a novel homozygous nonsense mutation in the GTF2H5 gene. J Dermatol. 2014;41(8):705–8.

46. Giglia-Mari G, Coin F, Ranish JA, Hoogstraten D, Theil A, Wijgers N, Jaspers NG, Raams A, Argentini M, van der Spek PJ, et al. A new, tenth subunit of TFIIH is responsible for the DNA repair syndrome trichothiodystrophy group A. Nat Genet. 2004;36(7):714–9.

47. Faghri S, Tamura D, Kraemer KH, Digiovanna JJ. Trichothiodystrophy: a systematic review of 112 published cases characterises a wide spectrum of clinical manifestations. J Med Genet. 2008;45(10):609–21.

48. Wortmann SB, Vaz FM, Gardeitchik T, Vissers LE, Renkema GH, Schuurs-Hoeijmakers JH, Kulik W, Lammens M, Christin C, Kluijtmans LA, et al. Mutations in the phospholipid remodeling gene SERAC1 impair mitochondrial function and intracellular cholesterol trafficking and cause dystonia and deafness. Nat Genet. 2012;44(7):797–802.

49. Tort F, Garcia-Silva MT, Ferrer-Cortes X, Navarro-Sastre A, Garcia-Villoria J, Coll MJ, Vidal E, Jimenez-Almazan J, Dopazo J, Briones P, et al. Exome sequencing identifies a new mutation in SERAC1 in a patient with 3-methylglutaconic aciduria. Mol Genet Metab. 2013;110(1–2):73–7.

50. Maas RR, Iwanicka-Pronicka K, Kalkan Ucar S, Alhaddad B, AlSayed M, Al-Owain MA, Al-Zaidan HI, Balasubramaniam S, Baric I, Bubshait DK, et al. Progressive deafness-dystonia due to SERAC1 mutations: a study of 67 cases. Ann Neurol. 2017;82(6):1004–15.

51. Carroll J, He J, Ding S, Fearnley IM, Walker JE. TMEM70 and TMEM242 help to assemble the rotor ring of human ATP synthase and interact with assembly factors for complex I. Proc Natl Acad Sci USA. 2021;118(13):e2100558118.

52. Sanders SS, Hernandez LM, Soh H, Karnam S, Walikonis RS, Tzingounis AV, Thomas GM. The palmitoyl acyltransferase ZDHHC14 controls Kv1-family potassium channel clustering at the axon initial segment. Elife. 2020;9:e56058.

53. Yarar D, Waterman-Storer CM, Schmid SL. SNX9 couples actin assembly to phosphoinositide signals and is required for membrane remodeling during endocytosis. Dev Cell. 2007;13(1):43–56.

Lu *et al. BMC Medical Genomics*   (2021) 14:270

Page 14 of 14

54. Lopez LM, Harris SE, Luciano M, Liewald D, Davies G, Gow AJ, Tenesa A, Payton A, Ke X, Whalley LJ, et al. Evolutionary conserved longevity genes and human cognitive abilities in elderly cohorts. Eur J Hum Genet: EJHG. 2012;20(3):341–7.

55. Nagamani SC, Erez A, Eng C, Ou Z, Chinault C, Workman L, Coldwell J, Stankiewicz P, Patel A, Lupski JR, et al. Interstitial deletion of 6q25.2-q25.3: a novel microdeletion syndrome associated with microcephaly, developmental delay, dysmorphic features and hearing loss. Eur J Hum Genet: EJHG. 2009;17(5):573–81.

56. Paulraj P, Palumbos JC, Openshaw A, Carey JC, Toydemir RM. Multiple congenital anomalies and global developmental delay in a patient with interstitial 6q25.2q26 deletion: a diagnostic odyssey. Cytogenet Genome Res. 2018;156(4):191–6.

57. Michelson M, Ben-Sasson A, Vinkler C, Leshinsky-Silver E, Netzer I, Frumkin A, Kivity S, Lerman-Sagie T, Lev D. Delineation of the interstitial 6q25 microdeletion syndrome: refinement of the critical causative region. Am J Med Genet Part A. 2012;158A(6):1395–9.

58. Pirola B, Bortotto L, Giglio S, Piovan E, Janes A, Guerrini R, Zuffardi O. Agenesis of the corpus callosum with Probst bundles owing to haploinsufficiency for a gene in an 8 cM region of 6q25. J Med Genet. 1998;35(12):1031–3.

59. Shen-Schwarz S, Hill LM, Surti U, Marchese S. Deletion of terminal portion of 6q: report of a case with unusual malformations. Am J Med Genet. 1989;32(1):81–6.

60. Ronzoni L, Tagliaferri F, Tucci A, Baccarin M, Esposito S, Milani D. Interstitial 6q25 microdeletion syndrome: ARID1B is the key gene. Am J Med Genet Part A. 2016;170A(5):1257–61.

61. Peter B, Lancaster H, Vose C, Fares A, Schrauwen I, Huentelman M. Two unrelated children with overlapping 6q25.3 deletions, motor speech disorders, and language delays. Am J Med Genet Part A. 2017;173(10):2659–69.

62. De Crescenzo A, Citro V, Freschi A, Sparago A, Palumbo O, Cubellis MV, Carella M, Castelluccio P, Cavaliere ML, Cerrato F, et al. A splicing mutation of the HMGA2 gene is associated with Silver-Russell syndrome phenotype. J Hum Genet. 2015;60(6):287–93.

63. Fischer-Zirnsak B, Segebrecht L, Schubach M, Charles P, Alderman E, Brown K, Cadieux-Dion M, Cartwright T, Chen Y, Costin C, et al. Haploinsufficiency of the notch ligand DLL1 causes variable neurodevelopmental disorders. Am J Hum Genet. 2019;105(3):631–9.

64. Kamelgarn M, Chen J, Kuang L, Jin H, Kasarskis EJ, Zhu H. ALS mutations of FUS suppress protein translation and disrupt the regulation of nonsense-mediated decay. Proc Natl Acad Sci USA. 2018;115(51):E11904–13.

65. Yan Q, Weyn-Vanhentenryck SM, Wu J, Sloan SA, Zhang Y, Chen K, Wu JQ, Barres BA, Zhang C. Systematic discovery of regulated and conserved alternative exons in the mammalian brain reveals NMD modulating chromatin regulators. Proc Natl Acad Sci USA. 2015;112(11):3445–50.

66. Shyu AB, Wilkinson MF, van Hoof A. Messenger RNA regulation: to translate or to degrade. EMBO J. 2008;27(3):471–81.

67. Celen C, Chuang JC, Luo X, Nijem N, Walker AK, Chen F, Zhang S, Chung AS, Nguyen LH, Nassour I, et al. Arid1b haploinsufficient mice reveal neuropsychiatric phenotypes and reversible causes of growth impairment. Elife. 2017;6:e25730.

68. Shibutani M, Horii T, Shoji H, Morita S, Kimura M, Terawaki N, Miyakawa T, Hatada I. Arid1b haploinsufficiency causes abnormal brain gene expression and autism-related behaviors in mice. Int J Mol Sci. 2017;18(9):1872.

69. Ellegood J, Petkova SP, Kinman A, Qiu LR, Adhikari A, Wade AA, Fernandes D, Lindenmaier Z, Creighton A, Nutter LMJ, et al. Neuroanatomy and behavior in mice with a haploinsufficiency of AT-rich interactive domain 1B (ARID1B) throughout development. Mol Autism. 2021;12(1):25.

Publisher's Note